Design and Simulation of a Vapour Compression Refrigeration System Using Phase Change Material

Raju Siddharth[1*], *Korody Jagannath*[2], *Kini Giridhar P.*[3] and *K. Kedlaya Vishnumurthy*[4]

[1] *Department of Electronics and Communications Engineering, Manipal Institute of Technology, Manipal Academy of Higher Education, Manipal, India*
[2] *Department of Mechanical and Manufacturing Engineering, Manipal Institute of Technology, Manipal Academy of Higher Education, Manipal, India*
[3] *Department of Electrical and Electronics Engineering, Manipal Institute of Technology, Manipal Academy of Higher Education, Manipal, India*
[4] *Department of Electronics and Communications Engineering, Manipal Institute of Technology, Manipal Academy of Higher Education, Manipal, India*

Abstract. The paper details the design and simulation of a solar powered vapour compression refrigeration system. The effect of a phase change material, in this case ice, on a vapour compression refrigeration system powered by solar panels is discussed. The battery and solar panels were sized to allow the system to function as an autonomous unit for a minimum of 12 hours. It was concluded that the presence of a phase change material in the refrigeration system caused a considerable increase in both the on and off time of the compressor. The ratio by which the on time increased was greater than the ratio by which the off time was increased. There was a 219% increase in the on time, a 139% increase in the compressor off time and a 3.5% increase in compressor work accompanied by a 5.5% reduction in COP. Thus, under conditions where there is enough load in the system to cause the initial on and off times of the compressor to be comparable, the presence of a phase change material may result in a greater on period than an off period for the compressor.

1 Introduction

On average nearly 300 days a year in India are sunny[1], with about 1,500–2,000 sunshine hours per year depending upon location. The daily average solar energy incident over India varies between 4 to 7 kWh/m^2[1]. This provides huge potential for projects that use solar energy to be implemented. Although there has been considerable progress in this field, a lot of scope remains to rework and improve existing ways of utilizing solar energy in a viable manner. At the same time, there is also room for creation of new ways to efficiently engage with solar power.

* Corresponding author: siddharth.raju94@gmail.com

Many vaccines such as polio vaccines are temperature sensitive and must be stored in storage units with controlled temperatures. In regions that experience irregular supply of electricity, the project may have potential to store vaccines at the desired temperatures. The project aims to describe the design and simulation of a solar powered vapour compression refrigeration system employing a phase change material. The constraints of this system were defined by its application, the storage of vaccines. The components of the system included solar panels, a maximum power point tracking unit, a battery bank, vapour compression refrigeration system. The system was simulated using Matlab/Simulink. Each component was sized and configured appropriately in order to optimise the performance of the system. The battery and solar panels where sized to allow the system to function as an autonomous unit for a minimum of 12 hours. The characteristic curves of SSI150W solar panels by Solar India were simulated and studied.

2 Literature Review

Mba E.F. et al. [2] (2012) developed a mathematical model of a solar vapour compression system and simulated the photovoltaic modules using MATLAB. The designed system consisted of a vapour compression refrigerator, solar panels, solar charge controller, a DC inverter and a lead acid battery. The relationship between solar radiation intensity and temperature attained in the refrigerator was studied. Different photovoltaic models were analysed and their characteristic curves were studied. No power was produced by the panel under short circuit and open circuit conditions. The open circuit voltage remained constant with an increase in solar irradiation while the short circuit current increased linearly. It was also noted that the power produced by the panels had a unique operating point at which power produced was maximum. It was concluded that with an increase in load current, there was a non-linear decrease in the panel voltage.

Kalbande and Deshmukh [3,4] (2015,2016) constructed a PV based vapour compression refrigeration system for vaccine preservation. The desired temperature to be maintained in the storage unit was 2℃ to 8℃.The model was implemented using a DC vapour compression refrigerator of 25 litre capacity, two 80 W PV panels connected in parallel with 35° tilt angle, a 12 V – 150Ah sealed lead acid battery and a charge controller. It was observed that the average PV conversion efficiency was 8.5% and PV exergy efficiency was 11% in both no load and full load conditions. This indicated that load conditions of the refrigeration system do not affect the PV system.

Del Pero et al. [5] (2015) conducted a feasibility study for a solar refrigeration kit for remote areas in developing countries. A system consisting of PV panels, a refrigeration unit and a controller was designed with an additional aim that the thermally insulated envelope equipped with an energy storage system could be designed on site using local materials. An energy model was defined and simulation was carried out to identify the optimal size of the refrigerated volume, energy storage and the PV section. It was observed that there was a surplus of energy generated by the panel when compared with compressor power consumption. However, the excess power produced remained unutilized. It was also estimated that the cost of the system would be 500 Euro.

Alkelani and Kanyarusoke [6] (2016) designed and constructed an inverter-less solar assisted refrigeration system for the storage of fruits and vegetables. The system consisted of 12-volt PV panels, a battery bank, charge controller and a DC vapour compression refrigerator. The desired temperature to be maintained was between 5℃ and 15℃. The PV system was sized according to the refrigeration system requirements. The solar radiation on the PV panels was estimated using the Perez model, as the panels were tilted. It was observed that the total solar irradiation on an inclined PV panel was greater than the solar irradiation on a horizontal surface. The size of the refrigerator components was computed on the heat

loads of the system. The system was tested without load and then with 20kg of fruits. It was concluded that the system was able to maintain the desired temperature, with the overall COP based on the input to the panels being 2.8.

It can be concluded from the literature review, that a solar powered refrigeration system should consist of the following components: PV panels, charge controller, battery bank and a vapour compression system. If an AC compressor is used in the system an inverter will be required to convert the direct current produced by panels to alternating current that will be fed to the refrigerator. This can be avoided by the use of a DC compressor. The sizing of the battery bank and the PV array depends on the expected time the refrigerator has to run however it is independent of the load present in the refrigerator at a given time.

3 Methodology

3.1 Refrigeration System

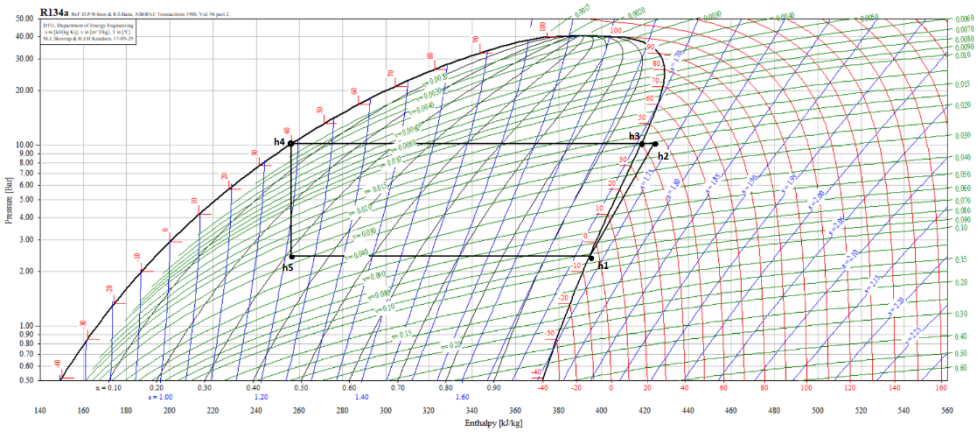

Fig.1 P-H Diagram for a Vapour Compression Refrigeration System.

A single stage vapour compression refrigeration system has was considered and modelled for the simulation. Refrigeration is obtained as the refrigerant evaporates at a low temperature and pressure. It employs a compression process to raise the pressure and temperature of the refrigerant. The refrigerant then flows through a condenser at higher pressure, then through a throttling device, and then back to low pressure, in the evaporator.

Evaporator Unit [2,4,7,8]: It consists of coils of pipe through which the refrigerant flows at low pressure and temperature. The refrigerant is maintained at a lower temperature than the surrounding medium, thus absorbing the latent heat of evaporation required from the medium to be cooled. Heat transfer rate at evaporator $\dot{Q}_e$ is given by:

$$\dot{Q}_e = \dot{m}\mathrm{R} \tag{1}$$

$$\dot{Q}_e = \dot{m}(\mathrm{h_1} - \mathrm{h_5}) \tag{2}$$

Where:
$\dot{m}$: Mass flow rate of refrigerant (kg/s)
R: The refrigeration effect, which is equal to the heat transferred at the evaporator per kilogram of refrigerant.
$\mathrm{h_1}$: Specific enthalpy at the exit of the evaporator (kJ/kg)
$\mathrm{h_7}$: Specific enthalpy at the inlet of the evaporator (kJ/kg)

Compressor Unit [2,4,7,8]: It maintains the desired evaporator pressure corresponding to the requirement of low temperature. It continuously draws the refrigerant vapour from the evaporator, allowing low pressure and temperature to be maintained in the evaporator. The compressor also raises the pressure and temperature of the refrigerant so that it can reject heat to the external environment in the condenser. Power input to the compressor $\dot{W}_c$, is given by:

$$\dot{W}_c = \dot{m}W \tag{3}$$

$$\dot{W}_c = \dot{m}(\mathrm{h_2\text{-}h_1}) \tag{4}$$

where:
W: The work done by the compressor, which is equal to the work input to the compressor per kilogram of refrigerant.
$\mathrm{h_2}$: Specific enthalpy at the outlet of the compressor (kJ/kg)

Condenser unit [2,4,7,8]: In this unit, the heat absorbed in the evaporator and the heat added in the compressor to the refrigerant is rejected to the external environment, resulting in the condensation of the refrigerant. Heat transfer rate at condenser $\dot{Q}_c$, is given by

$$\dot{Q}_c = \dot{m}(h_3\text{-}\, h_4) \tag{5}$$

where
$\mathrm{h_3}$: Specific enthalpy at the inlet of the condenser (kJ/kg)
$\mathrm{h_4}$: Specific enthalpy at the outlet of the condenser (kJ/kg)

Expansion Device [2,4,7,8]: It restricts the flow of the refrigerant leading to a pressure drop, resulting in a throttling process. Thus reducing the pressure of the refrigerant. For the isenthalpic expansion process:

$$\mathrm{h_4 = h_5} \tag{6}$$

Coefficient of Performance [6-8]: The COP of the system is given by:

$$\mathrm{COP} = \frac{\dot{Q}_e}{\dot{W}_c} = \frac{\dot{m}(\mathrm{h_1 - h_5})}{\dot{m}(\mathrm{h_2 - h_1})} = \frac{(\mathrm{h_1 - h_5})}{(\mathrm{h_2 - h_1})} \tag{7}$$

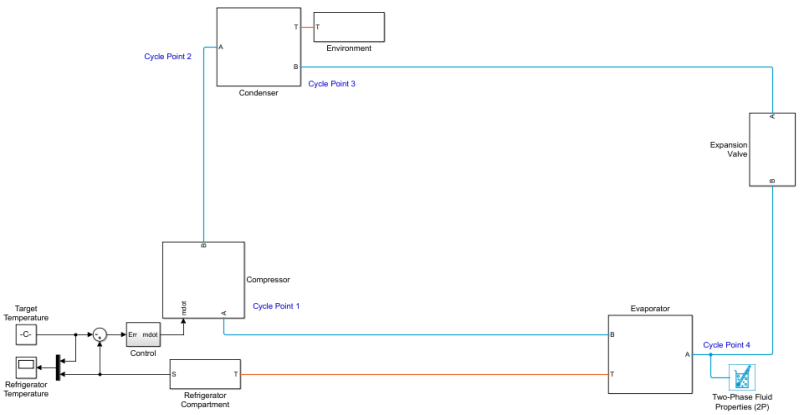

Fig. 2. Modelling the Refrigeration System.

3.2 Heat Transfer in Cooling Chamber

The sensible heat Q present in the cooling chamber can be estimated by [5-8]:

$$Q=mc_p\Delta T \tag{8}$$

Where
m = Mass of vaccines (kg)
c_p = Specific heat of medium (kJ/kgK)
ΔT = Change in temperature of cooling chamber (K)

Assuming the walls of the chamber are composite walls, the heat transfer can be estimated by [6-8]:

$$\frac{Q}{A}=\frac{\Delta T}{(\frac{L_1}{K_1}+\frac{L_2}{K_2}+\frac{L_3}{K_3})} \tag{9}$$

Where:
Q: Heat transfer (W)
A: Surface area of refrigerator (m^2)
ΔT = Difference in temperature between external environment and cooling chamber (K)
L: Length of walls (m)
K: Thermal conductivity (W/mk)

The compressor ON and OFF time can be determined using the following equations [9]:

$$Q_i + Q_1 = Q_f \tag{10}$$

During compressor OFF time:

$$Q_1 = t_{off} * W_1 \tag{11}$$

Where
Q_i: Energy content of the chamber at the end of the ON duration (kJ)
Q_f: Energy content of the chamber at the end of the OFF duration (kJ)
t_{off}: Compressor OFF time duration/cycle (s)
W_1: Average heat transfer rate from external environment to cooling chamber (kJ/s)

$$mc_p\Delta T= Q_f - Q_i \tag{12}$$

$$mc_p\Delta T=t_{off} * W_1 \tag{13}$$

During compressor ON time assuming W_1 remains constant for both ON and OFF time

$$Q_e = (Q_f - Q_i) + Q_2 \tag{14}$$

$$Q_e = t_{on} * W_e \tag{15}$$

$$Q_2= t_{on} * W_1 \tag{16}$$

Where
W_e: Evaporator capacity (kJ)
t_{on}: Compressor ON time duration/cycle (s)

$$(Q_f - Q_i) = Q_e - Q_2 \tag{17}$$

$$\mathrm{m}c_p \Delta T = t_{on}(W_e - W_1) \tag{18}$$

3.3 Phase Change Material

Most temperature sensitive vaccines are required to be stored at temperatures between 2°C to 8°C. Under these constraints the desired PCM should ideally have a melting point, within the desired temperature range. Thus, paraffin wax consisting of mixtures of n-Tetradecane was considered as they have a melting point near 6°C. However, based on cost and ease of availability, ice was chosen as the desired phase change material. It was desired that the phase change material provides the same cooling effect as the evaporator coil for an estimated amount of time. The mass of ice required by the system can be estimated by the following equation [7]:

$$Q_{ice} = Q_e = m_{ice}(C_s \int_{T_1}^{0} dT + L + C_f \int_{0}^{T_2} dT) \tag{19}$$

Where
Q_e: Heat removed by the evaporator (kJ)
m_{ice}: Mass of ice (Kg)
C_s: Specific heat of ice (kJ/kgK)
C_f: Specific heat of water (kJ/kgK)
L: latent heat of fusion (kJ/kg)
T_1: Initial temperature of ice (K)
T_2: Final temperature of ice (K)

3.4 Sizing of Battery and PV module

Having calculated the power being consumed by the compressor, the capacity C of the battery in ampere hours can be estimated using the following equation [8,10,11]:

$$\mathrm{C}= \frac{Daily\ power\ consumed * Days\ of\ autonomity * Battery\ operation\ period}{Nominal\ Voltage * Depth\ of\ Discharge * Corrective\ Factor} \tag{20}$$

Similarly, PV module size can also be estimated by:

$$\mathrm{P}= \frac{Daily\ power\ consumed * Battery\ operation\ period}{Sunlight\ hours * Depth\ of\ Discharge * Corrective\ Factor} \tag{21}$$

3.5 Photovoltaic Cell

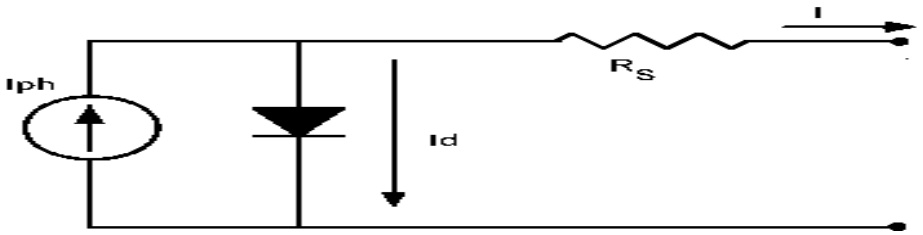

Fig.3. Equivalent PV cell circuit

Table. 1. Solar Panel SSI150W

Power	150 W
Nominal Voltage	12 V
Open Circuit Voltage	21.6 V
Short Circuit Current	9.21 A
Maximum Power Point Voltage	17.3 V
Maximum Power Point Current	8.67 A
Number of Cells	36

The panels have been modelled on the basis of a single diode, series resistance model of a solar panel. The panel selected for the purpose of the project were Solar India 150 W 12 V Polycrystalline Solar Panel SSI150W. The model was simulated on Matlab/Simulink, under conditions of constant solar radiation intensity and varying module temperature. Then under conditions of constant temperature and varying solar radiation intensity. The configuration of the PV cell can be mathematically by [12-18]:

$$I=I_{ph}-I_d \tag{22}$$

$$I_d = I_0\left[e^{\frac{V+I.R_S}{a}}-1\right] \tag{23}$$

$$I_{ph}=\frac{G}{G_{ref}}\left(I_{ph,ref}+\mu_{sc}*\Delta T\right) \tag{24}$$

$$I_{0,ref}=I_{sc,ref}\left[e^{\frac{-V_{oc}}{a_{ref}}}\right] \tag{25}$$

The final output current for N_p parallel cells present in the array, is determined by:

$$I=N_p*I_{ph}-N_p*I_d\{e^{[\frac{q}{K*N_S*A*T_{op}}*(V+I*R_S)]}-1\} \tag{26}$$

Where:
V= k*T_c/q

a= $(N_s * A * k * T_c)/q$
I_{ph}: the photocurrent (A)
I_d: the diode current (A)
I_0: The reverse saturation or leakage current of the diode (A)
T_c: The operating temperature of the cell (K)
k: Boltzmann constant= $1.381 \cdot 10^{-23}\ J/K$
q: Electron charge = $1.602 \cdot 10^{-19}$ C
N_s: Number of PV cells connected in series.
A: the ideality factor
G: Irradiance (W/m^2)
G_{ref}: Irradiance at STC (W/m^2)
μ_{sc}: Coefficient temperature of short circuit current (A/K)
ΔT: $T_c - T_{c,ref}$ (K)
$T_{c,ref}$: Cell temperature at STC (K)
D: Diode diffusion factor
ε_G: Material band gap energy (eV)

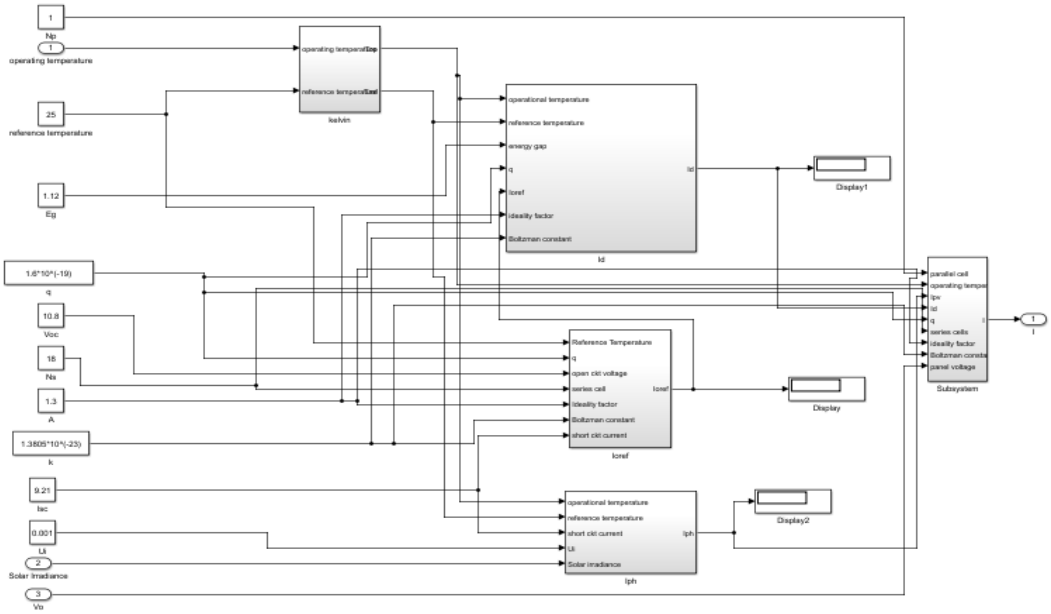

Fig. 4. Modelling of PV Subsystem.

3.6 MPPT using Perturb and Observe Algorithm

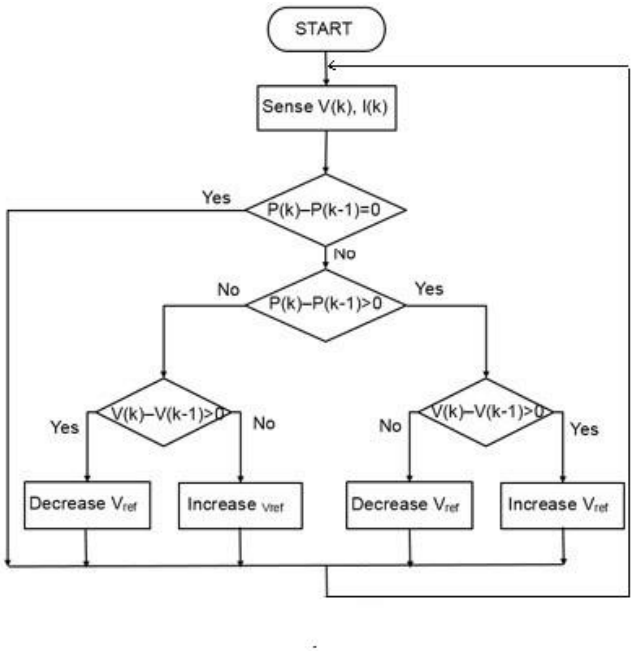

Fig. 5. P&O Algorithm.

A Maximum Power Point tracking unit [19-22] allows optimum power to be transferred from the PV module to the load under given atmospheric conditions. The converter acts as a load to the PV module. Altering the duty cycle results in the variation of impedance of the converter circuit. By the maximum power transfer theorem when the impedance of the converter will be similar to the internal impedance of the cell under given conditions, maximum power will be transferred. Based on the output of the PV module and the nominal voltage of the battery the duty cycle of the converter is varied using MPPT algorithms. The Perturb and Observe (P&O) algorithm [19-22] perturbs the operating voltage to ensure maximum power. The P&O algorithm reads the voltage and current produced by the solar photovoltaic array. It then calculates the power produced by the array. As can be seen from the characteristic PV curve of the solar module, the slope of the curve is positive to the left of the maximum power point and negative to the right. The power calculated at the instant 'k' is compared with the power calculated at the instant 'k-1' similarly the voltages at both these instances are also compared. If $dP/dV>0$, then it is known that the operating point is on the left side of the MPP. The P&O algorithm would increase the solar PV panel reference voltage to move the operating point towards the MPP. Alternatively, if the output voltage of the solar PV panels is perturbed and $dP/dV<0$, then it is known that the operating point is on the right side of the MPP. The P&O algorithm would decrease the solar PV panel reference voltage to move the operating point towards the maximum power point. When the steady state condition is touched the P&O technique oscillates around the maximum power point.

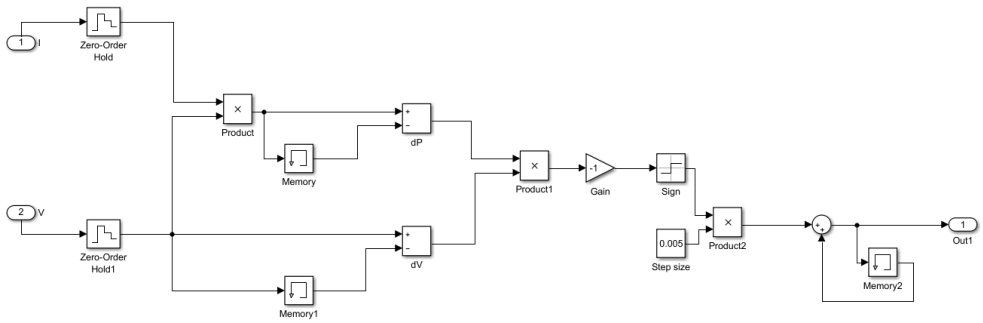

Fig. 6. Modelling the P&O Algorithm.

3.7 Buck-Boost Converter

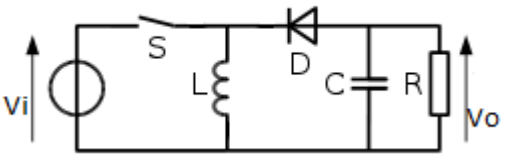

Fig. 7. Configuration of the Buck-Boost Converter

A buck boost converter [23] is a dc-dc converter that allows the output voltage to be either greater or lesser than the input voltage. When switch S is turned on, the diode D becomes reversed biased. Thus, the current flows through inductor L, charging it. When switch S is off the diode D becomes forward biased, resulting in the inductor discharging through capacitor C to the load. In this state, energy stored in the inductor is transferred to the load and the inductor current continues to fall till the switch S is turned on. The input and output voltage of the converter are related to the duty cycle of the switch by the following equation:

$$V_o = -\frac{DV_{in}}{(1-D)} \tag{27}$$

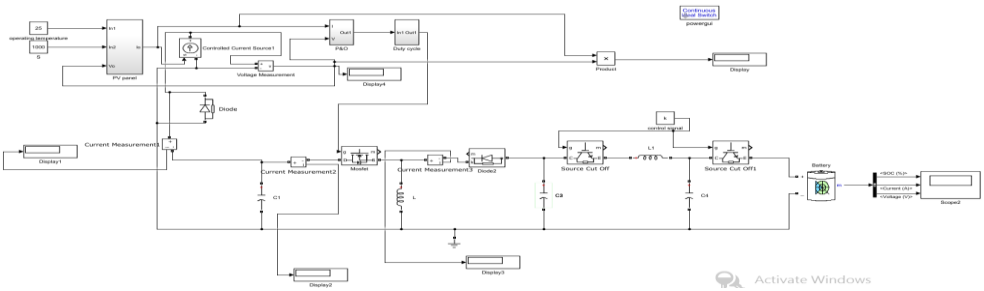

Fig. 8. MPPT using Buck-Boost Converter with Battery

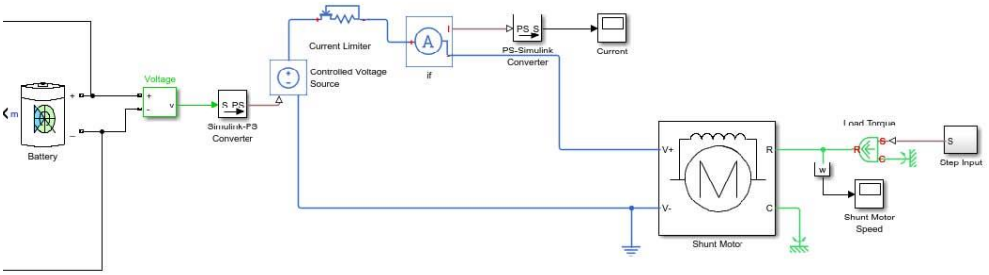

Fig. 9. Modelling of DC Shunt Motor Circuit.

3.8 Modelling of Systems

The subsystems have been designed and simulated in Matlab. The mechanical system is based on the example "Two-Phase Fluid Refrigeration" [24] available in the software. It has been designed using the thermodynamics library in Simscape. The PV module, MPPT unit and battery were simulated in Simulink. In addition, a shunt motor [25] was modelled in Simscape to verify that the solar panels could generate enough power to run the refrigeration system.

4 Results

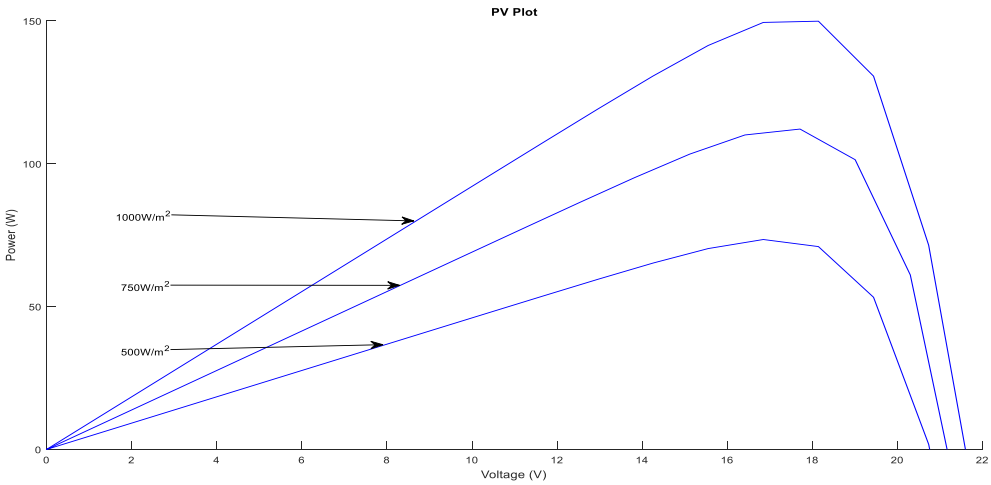

Fig. 10. Variation of Solar Irradiance at constant Temperature on P-V Characteristics of Solar Panel.

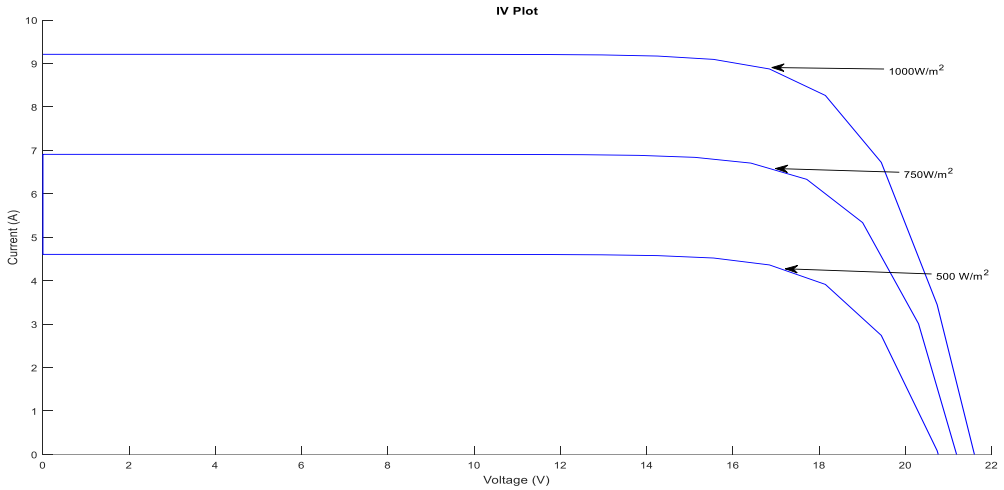

Fig. 11. Variation of Solar Irradiance at constant Temperature on I-V Characteristics of Solar Panel.

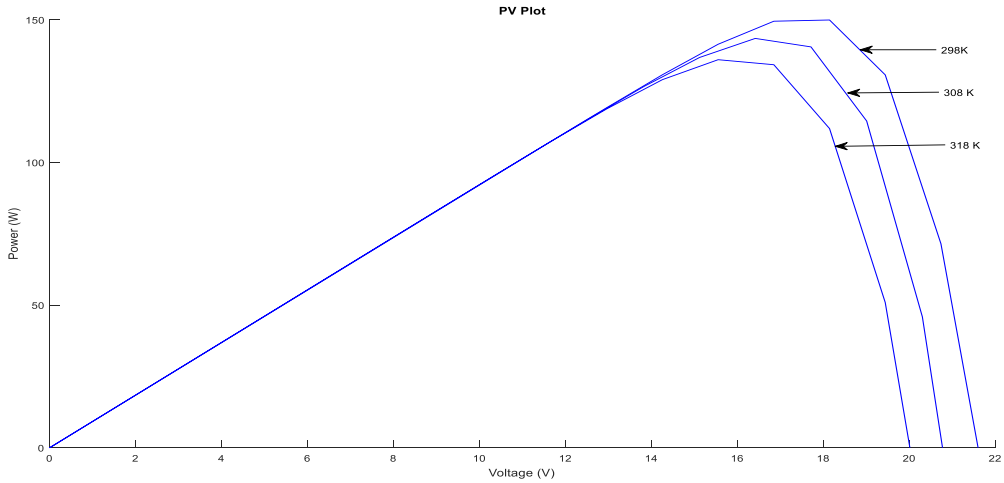

Fig. 12. Variation of Temperature at constant Solar Irradiation on P-V Characteristics of Solar Panel.

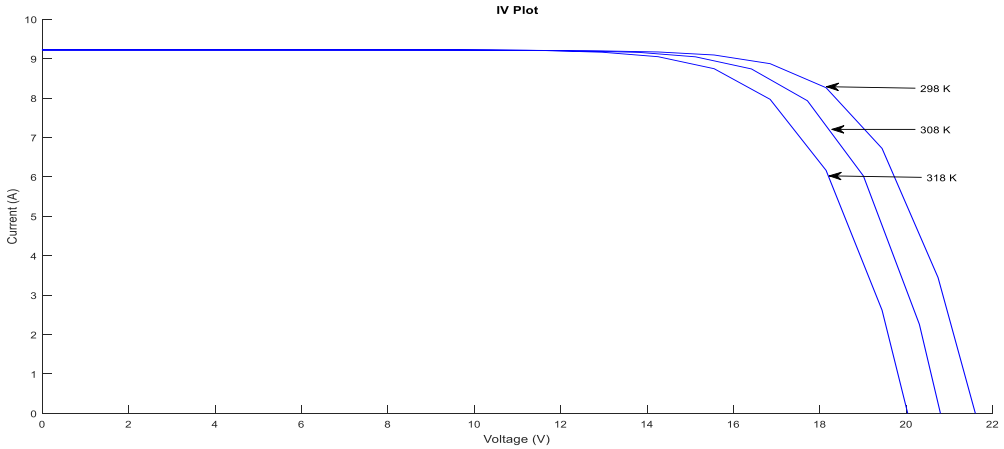

Fig. 13. Variation of Temperature at constant Solar Irradiation on P-V Characteristics of Solar Panel.

4.1 Simulation of Solar Panels

It was observed from the simulation of the solar panels that:

- Under conditions of varying irradiance at a constant temperature, there was a significant rise in module current with the rise in irradiance while the voltage increased at a much slower rate. There was an increase in module power with increase in solar irradiation.
- Under conditions of varying temperature at constant irradiance, with decreasing temperature, module current decreased slightly but PV voltage decreased significantly. There was an evident decrease in the output power of the PV cell with an increase in temperature.

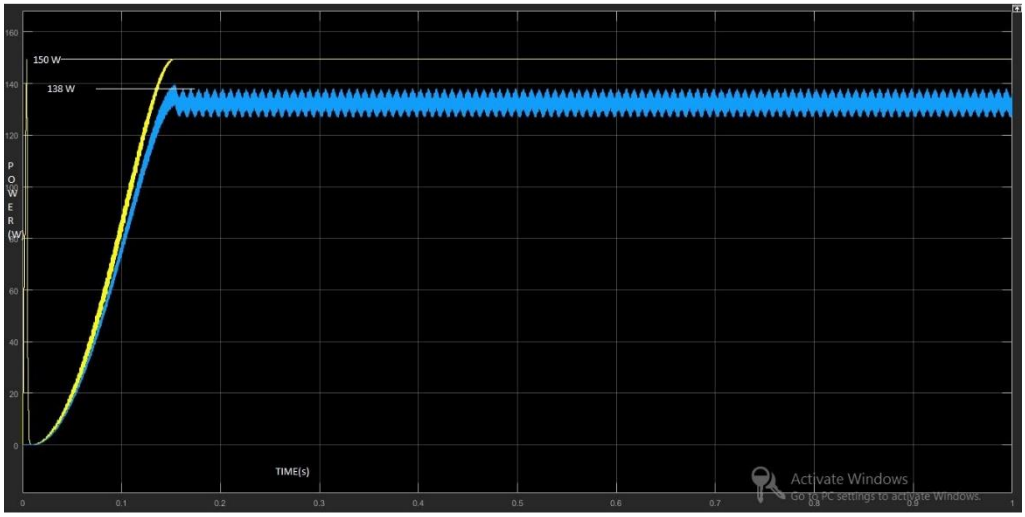

Fig. 14. Output Power of PV Module Compared with Output at DC-DC Converter.

4.2 Simulation of MPPT

It was observed during the simulation of the MPPT that:

- The P&O algorithm was followed and the unit tracked the output of the module. The output of the buck boost converter increased along with the panel power and then oscillated once steady state was achieved.
- While the module generated 150 W of power, there was loss of power at the output of the buck boost converter owing to switching losses, resistance of the components and forward voltage of diode.

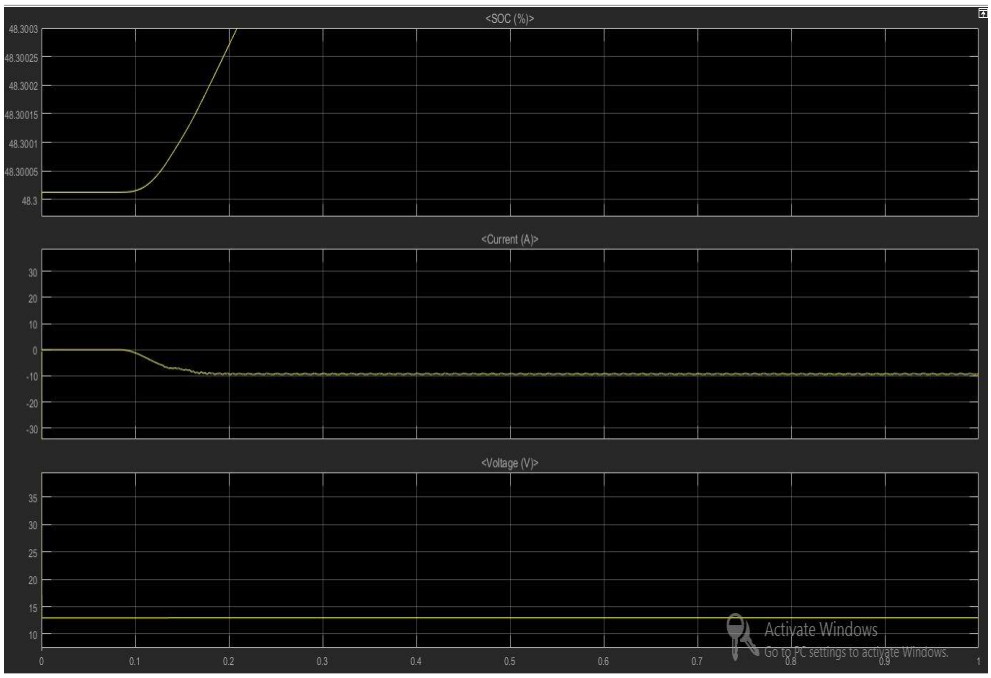

Fig. 15. Battery Parameters

4.3 Simulation of Battery Parameters

It was observed that with the presence of an MPPT unit most of the power generated by the panels was channelled to charge the battery. However, at the interface of the battery and the converter heavy interference was noted. Thus, an additional EMI filter was applied in order to reduce the noise. From the above simulation it was observed that approximately 129.5 W was transferred to the battery. This was in the form of a charging voltage of 12.95V with 10A of charging current.

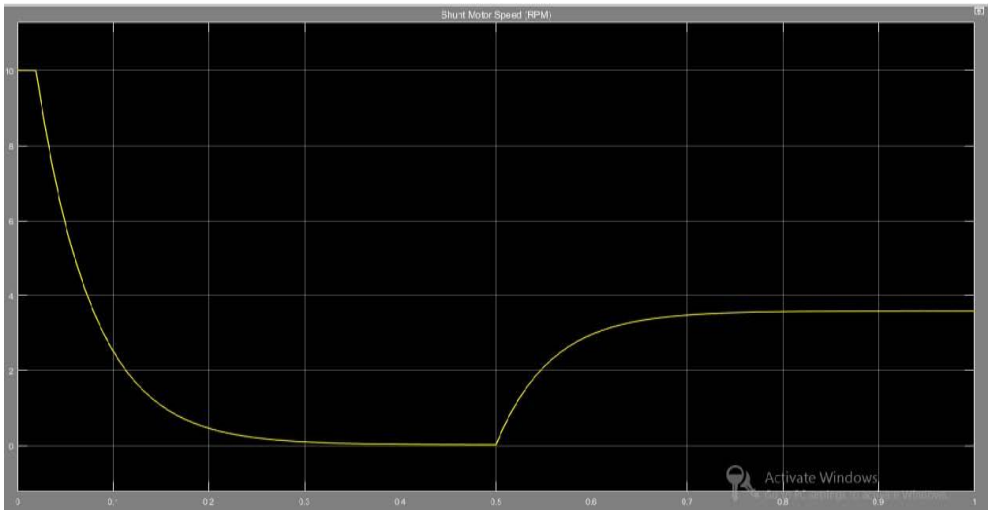

Fig. 16. DC Motor Current.

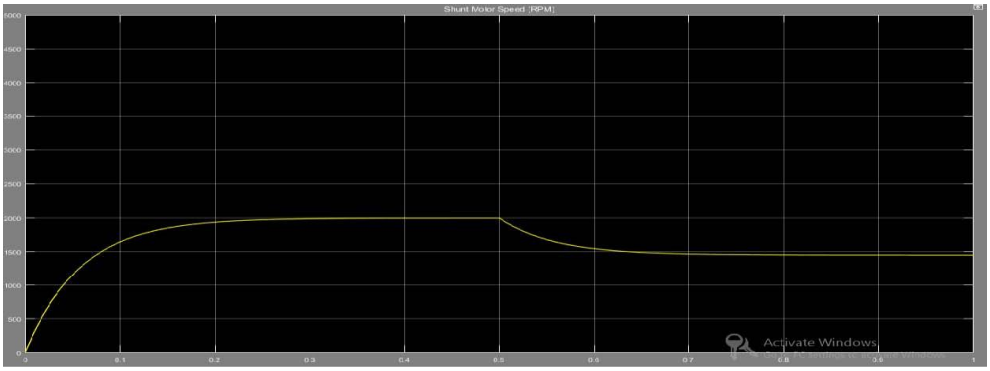

Fig. 17. DC Motor Speed.

4.4 Simulation of DC Motor

It was observed during the simulation of the DC motor that:

- With the aid of the current limiter the surge current was limited to 10 A. After the initial surge current was drawn, under zero load torque conditions the current drawn tended to zero. It is also noted that motor speed is at its highest under these conditions at 2000 rpm.
- As the load torque was increased there is an increase in the current drawn to 3.62 A, resulting in a speed of 1450 rpm and a power consumption of 43 W which was in line with the calculations for the maximum power drawn by the compressor.

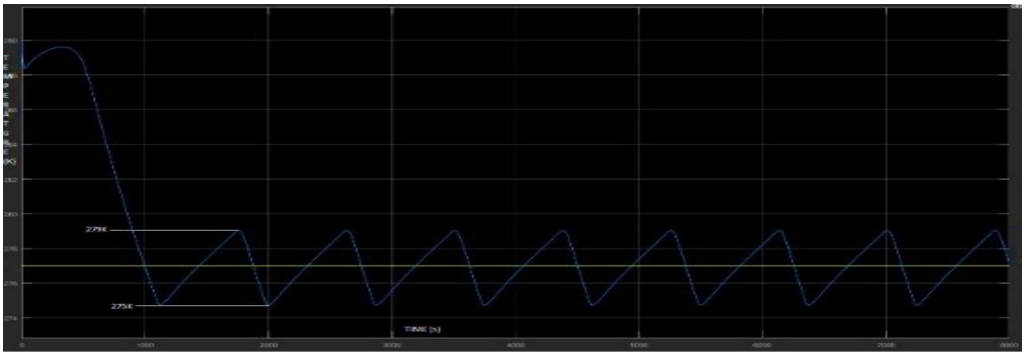

Fig. 18. Refrigerator Compartment Temperature without PCM.

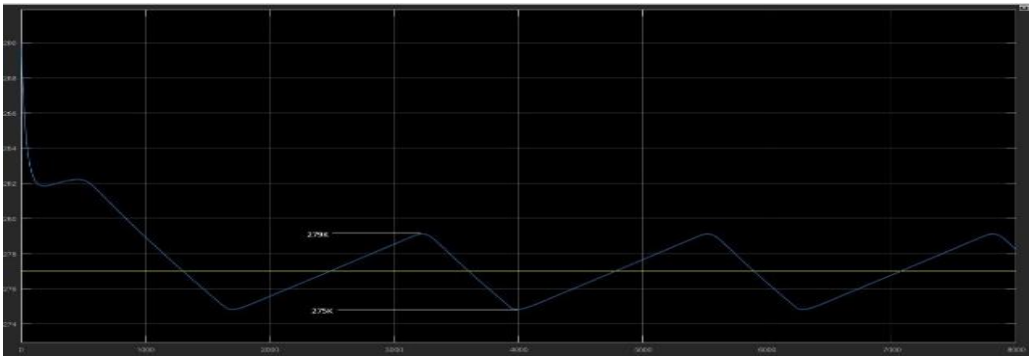

Fig. 19. Refrigerator compartment temperature with PCM.

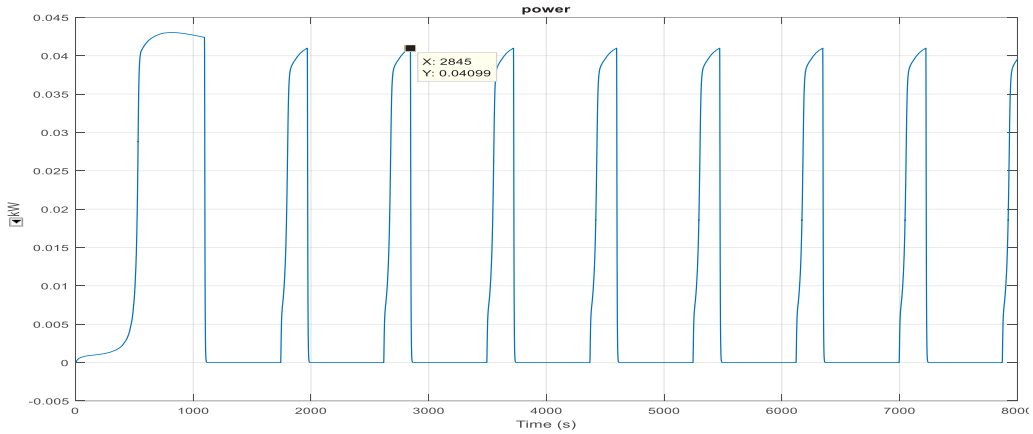

Fig. 20. Compressor Power Consumption Without PCM

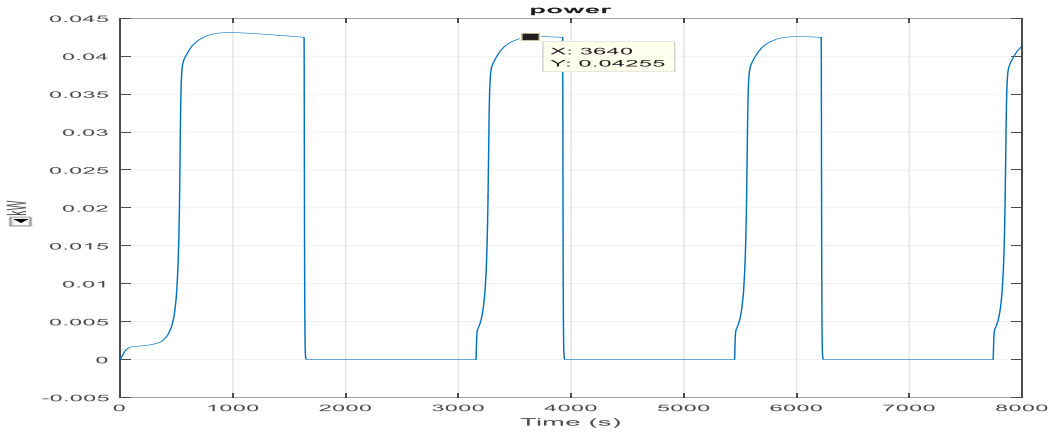

Fig. 21. Compressor Power Consumption With PCM.

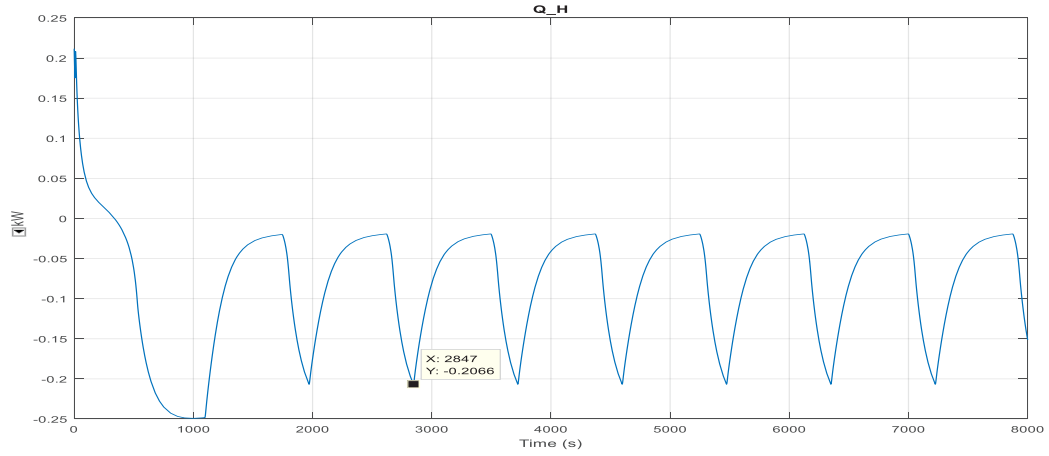

Fig. 22. Condenser Coil Capacity Without PCM

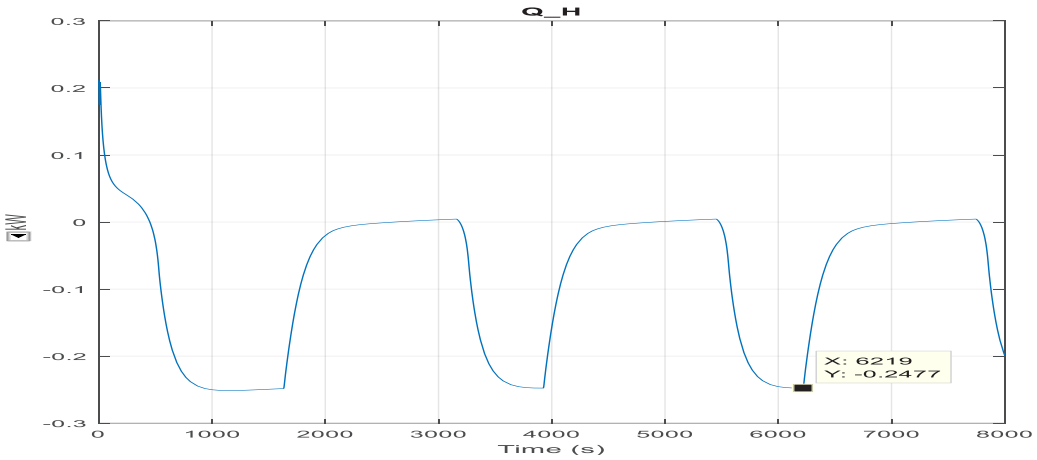

Fig. 23. Condenser Coil Capacity With PCM.

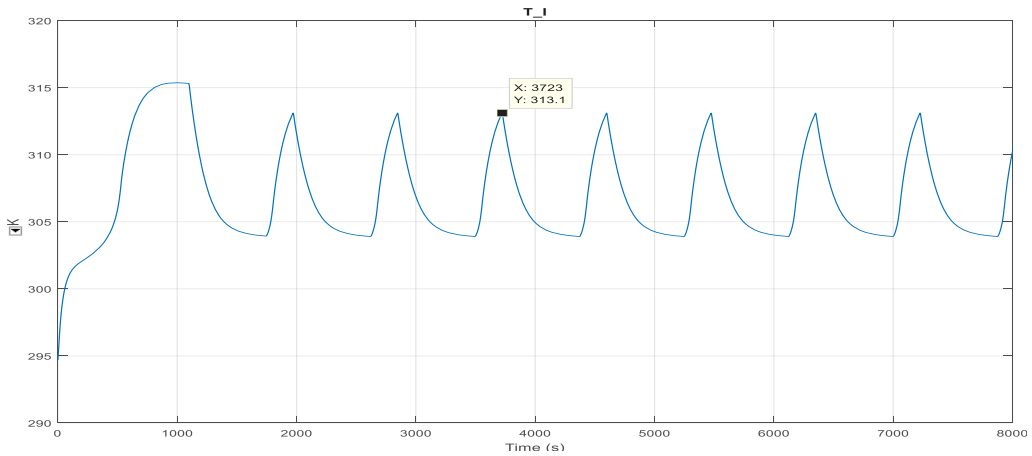

Fig. 24. Condenser Coil Temperature With PCM.

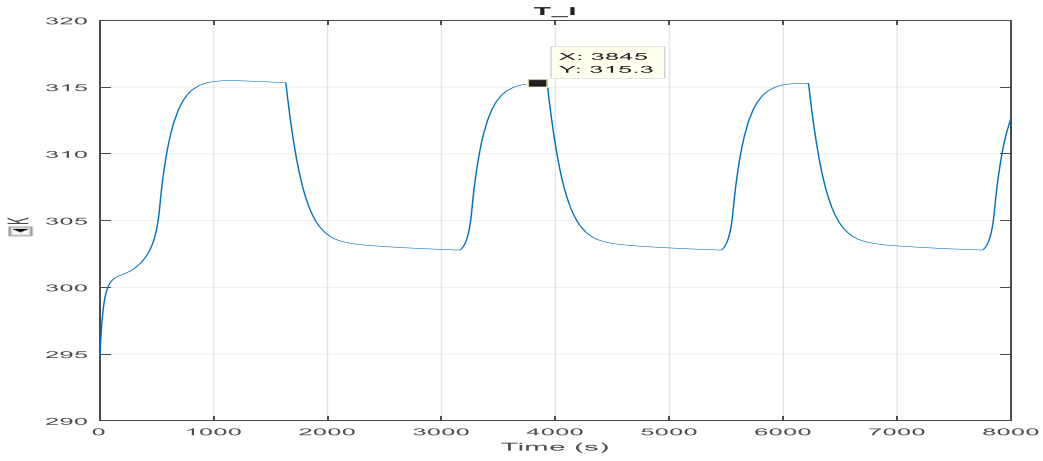

Fig. 25. Condenser Coil Temperature With PCM.

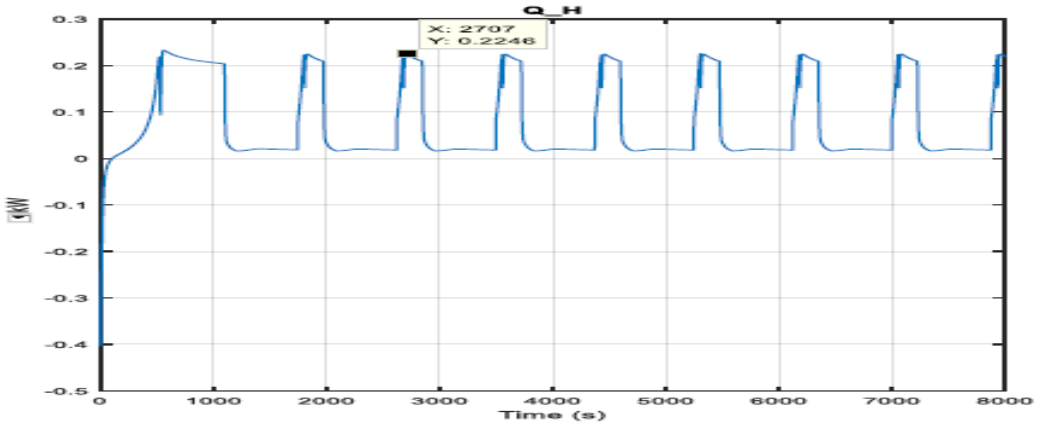

Fig. 26. Evaporator Coil Capacity Without PCM.

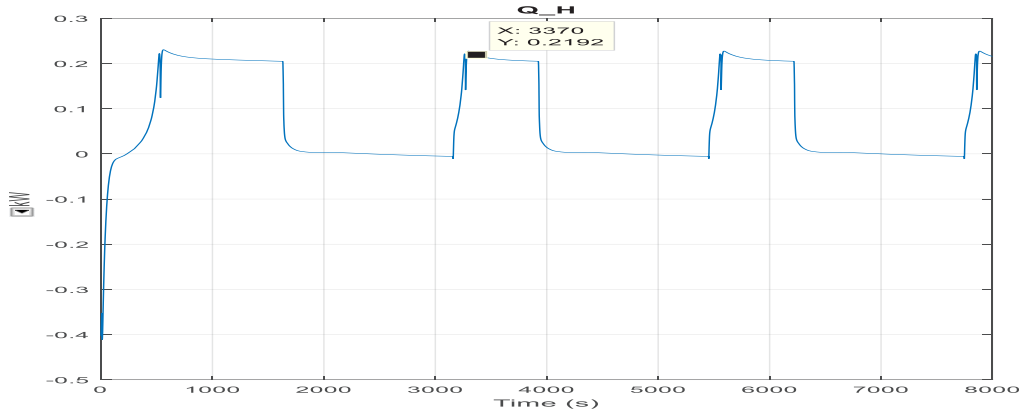

Fig. 27. Evaporator Coil Capacity With PCM.

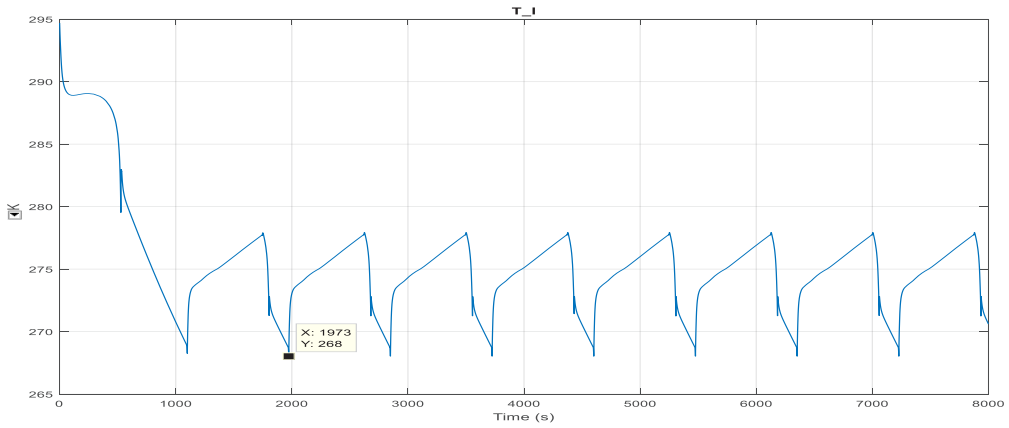

Fig. 28. Evaporator Coil Temperature Without PCM.

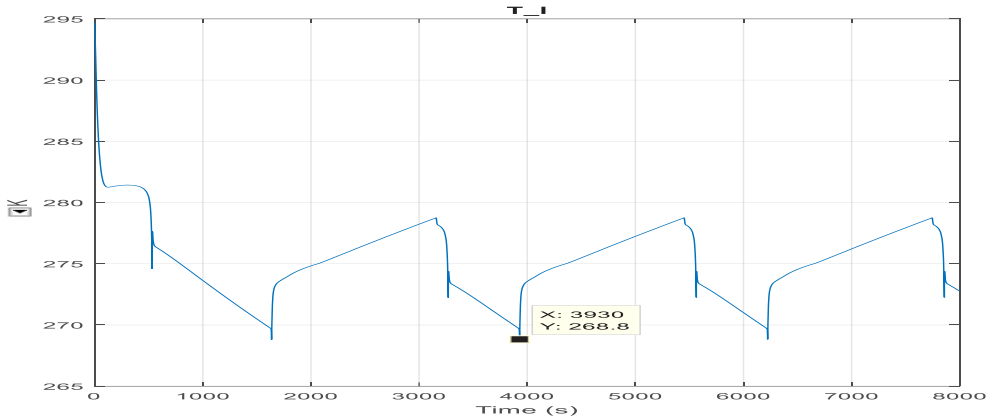

Fig. 29. Evaporator Coil Temperature With PCM

4.5 Simulation of Refrigeration Unit

Table. 2. Simulation of Refrigeration Unit

PCM	Power (Watt)	T_{on} (sec)	T_{off} (sec)	Evaporator Temp (K)	Evaporator Capacity (Watt)	Condenser Temp (K)	Condenser Capacity (Watt)	COP
Absent	41	249	627	268	224.6	313.1	207	5.48
Present	42.5	794	1500	268.8	219.2	315.3	248	5.16

It was noted in the simulation results of the refrigeration system using R134a refrigerant that:

- The presence of the phase change material increased both the on and off time of the compressor in a disproportionate manner as predicted by the theoretical calculations. There was a 219% increase in the on time, but only a 139% increase in the off time. There was a 5.8% fall in COP and a 3.5% increase in compressor work.
- The presence of the phase change material increased the minimum temperature to be maintained in the evaporator coil by 0.8 K. However, raised the temperature maintained in the condenser by 2.2 K.

6 Conclusions

The presented work aimed at designing and simulating a solar powered vapour refrigeration system using a phase change material. The project aimed at designing the system for the purpose of storing vaccines. The results of project have led to the following conclusions being drawn.

A system consisting of 150W panels with nominal voltage 12V, with the presence of a battery bank rated at 75Ah at nominal voltage 12V can successfully run a refrigeration system with rated at power consumption at 50W. As per theoretical calculations the system should be able to run as an autonomous unit for 12 hours at least, under the conservative estimate that only 6 hours of sunlight are present during the day. The battery bank provides enough charge for the system to run for 6 hours during which 50W is constantly consumed.

A single diode with series resistance model of a photovoltaic cell was implemented to validate the performance characteristics of solar panel SSI150W by Solar India. It was

observed with increasing PV module temperature, open circuit voltage decreased but short circuit current slightly increased, it was also observed that maximum power decreased with an increase in temperature. It was further observed that the open circuit voltage as well as the short circuit current increased with an increase in solar irradiation.

A maximum power point tracking unit was implemented using the Perturb and Observe algorithm and a buck boost converter. It was observed that the algorithm was able to track the maximum power point by altering the duty cycle of the buck boost converter. The output of the converter was observed and it was noted that the power oscillated after the maximum power point was found owing to the nature of the algorithm that requires constant perturbation of the voltage. It was also noted that the presence of a maximum power point tracking unit allowed greater charging current to be available for the battery.

It was concluded that the presence of a phase change material in the refrigeration system causes a considerable increase in both the on and off time of the compressor. This will aid in smooth running of the compressor without subjecting it to high temperature. However, the ratio by which the on time is increased is greater than the ratio by which the off time is increased. Numerically there is a 219% increase in the on time, a 139% increase in the compressor off time, a 5.8% fall in COP and a 3.5% increase in compressor work. Thus, under conditions where there is enough load in the system to cause the initial on and off times of the compressor to be comparable, the presence of a phase change material may result in a greater on period than an off period for the compressor. In terms of absolute value however the presence of ice in the refrigeration system does result in a significant increase in the off time. This implies that with the presence of ice as a PCM in the refrigeration system, a smaller battery bank would be required to operate the system. This increases the viability of using lower wattage solar panels to operate the same refrigeration system. Thus, reducing the overall cost of the system.

7 Future Work

There is scope to expand upon and further improve the presented work by:

- Employing alternate phase change materials, as the melting point of ice is 0°C and the maximum acceptable temperature for the storage of vaccines is 8°C. A phase change material, in particular, mixtures of n-Tetradecane which have a melting point near 6°C may perhaps provide better results.
- Varying the quantity of vaccine present in the cooling chamber would allow for a better understanding of how the ratio of PCM and load present in the refrigeration chamber affects the on and off time of the compressor.
- A major drawback arising from the current system is its inability to perform desired function in the prolonged absence of sunlight. In India this becomes relevant generally in the context of the monsoon season. While the occurrence of absolute absence of electricity is unlikely, it is possible to overcome such a situation by using hybrid systems to generate power.

References

1. Bala Bhaskar, *Energy Security and Economic Development in India: a Holistic Approach*, (TERI, 2013)
2. Mba E. F., Chukwuneke J. L., Achebe C. H. and Okolie P. C., JIEA, **2(10),** (2012)
3. S. R. Kalbande, Sneha Deshmukh, UJES, **3(2),** 17 (2015)

4. S. R. Kalbande, Sneha Deshmukh and V. P. Khambalkar, IJRANSS, **4(12),** 87 (2016)
5. C. Del Pero, F.M. Butera, M. Buffoli, L. Piegari, L. Capolongo and M. Fattore, ICCEP, 701 (2015)
6. Fouad M. Alkelani and Kant E. Kanyarusoke, ICUE, 178 (2016)
7. S. C. Arora & S. Domkundwar, *Refrigeration and Air-Conditioning*, (Dhanpat Rai Publication, 1992)
8. Armand Noël Ngueche Chedop, Noël Djongyang and Zaatri Abdelouahab, IJSR **3(11),** 1066 (2014)
9. Pradip Subramaniam, Chetan Tulapurkar,Ramasamy Thiyagarajan, G Thangamani, *Proceedings International Refrigeration and Air Conditioning Conference at Purdue*, (2010).
10. Sizing of Battery and PV module, Available from http://blog.su-kam.com, (9/3/2017)
11. Sizing of Battery and PV module, Available from http://www.leonics.com, (9/3/2017)
12. Ami Shukla, Manju Khare and K N Shukla, IJIRSET, **4(1),** 18516 (2015)
13. J. A. Ramos-Hernanz, J.J. Campayo, J. Larranaga, E. Zulueta, O. Barambones, J. Motrico, U. Fernandez Gamiz, I. Zamora, IJTPE, **4(10),** 45 (2012)
14. Habbati Bellia, Ramdani Youcef, Moulay Fatima, NRIAG, 53 (2014)
15. Jay Patel, Gaurag Sharma, IJRET, **2(3),** 225(2013)
16. Marcelo Gradella Villalva, Jonas Rafael Gazoli, and Ernesto Ruppert Filho, *IEEE Transactions on Power Electronics***, 24(5),** 1198 (2009)
17. M. G. Villalva, J. R. Gazoli, E. Ruppert F., SOBRAEP, **14(1),** 35(2009)
18. Chen Qi, Zhu Ming, *Physics Procedia*, **24,** 94 (2012)
19. Duy C. Huynh, Thu A. T. Nguyen, Matthew W. Dunnigan and Markus A. Mueller, ICIEA, 864 (2013)
20. A. Pradeep Kumar Yadav, S. Thirumaliah and G. Haritha, IJAREEIE, **1(1),** 18 (2012)
21. Aurobinda Panda, M. K. Pathak and S. P. Srivastava, IJETP, **1(2),** 18 (2011)
22. MPPT Algorithm, Available from https://www.mathworks.com, (13/4/2017)
23. Daniel W. *Hart, Power Electronics*, (Tata McGraw-Hill, 2011)
24. Two-Phase Fluid Refrigeration, Available from https://www.mathworks.com, (1/5/2017)
25. Shunt Motor, Available from https://www.mathworks.com, (18/5/2017)